AMERICAN SCIENTIFIC PUBLISHERS

Journal of Nanofluids
Vol. 4, pp. 394–401, 2015
(www.aspbs.com/jon)

ARTICLE

Unsteady Slip Flow of a Nanofluid Due to a Contracting Cylinder with Newtonian Heating

S. M. M. EL-Kabeir[1,2,*], Ali J. Chamkha[3], and A. M. Rashad[1]

[1]*Department of Mathematics, Aswan University, Faculty of Science, Aswan, 81528, Egypt*
[2]*Department of Mathematics, Salman bin Abdulaziz University, College of Science and Humanity Studies, AL-Kharj, 11942, Saudi Arabia*
[3]*Mechanical Engineering Department, Prince Mohammad Bin Fahd University, Al-Khobar 31952, Kingdom of Saudi Arabia*

In this paper, we analyzed the effects of partial slip on unsteady viscous flow and heat transfer of a nanofluid towards a contracting cylinder with Newtonian heating. The nanofluid model employed in the analysis includes the combined effects of Brownian motion and thermophoresis. Using appropriate similarity variables, the governing nonlinear partial differential equations have been transformed into a set of coupled nonlinear ordinary differential equations, which are solved numerically by an efficient implicit, iterative, finite-difference method. Graphical results for the dimensionless velocity, temperature, and nanoparticle concentration profiles are presented for various values of parameters controlling the flow regime. The expressions for the local skin friction coefficient, reduced Nusselt number, and the reduced Sherwood number are illustrated in tabular form and discussed quantitatively.

KEYWORDS: Nanofluid, Brownian Motion, Thermophoresis, Newtonian Heating, Contracting Cylinder, Partial Slip.

1. INTRODUCTION

The problems of flow and heat transfer in the boundary layer due to expanding or contracting surfaces have received great attention during the last decades owing to the abundance of practical applications in chemical and manufacturing processes. Examples of such technological processes are hot rolling, annealing and tinning of copper wires, glass-fiber, paper production, to name just a few. During the manufacture of these sheets, the melt issues from a slit and is subsequently stretched to achieve the desired thickness. The desired characteristics of the final product strictly depend on the rate of cooling and the process of stretching. It is therefore a great importance to know the flow behavior over a stretching surface which determines the rate of cooling. The basic stretching solutions include the flow due to the two-dimensional stretching surface was pioneered by Crane[1] and the axisymmetric radial stretching of a surface was considered by Wang.[2] Wang[3] also considered the fluid flow outside a stretching cylinder. Ishak et al.[4] have studied the forced convection on flow and heat transfer due to a stretching cylinder. Fang et al.[5] analyzed an unsteady viscous flow over an expanding or contracting cylinder. The unsteady viscous flow over a shrinking cylinder with mass transfer is studied by Zaimi et al.[6]

A nanofluid is a relatively new class of fluids which consist of a base fluid with nano-sized particles (1–100 nm), called nanoparticles. The nanoparticles used in nanofluids are typically made of metals, oxides, carbides, or carbon nanotubes. Conventional heat transfer base fluids such as oil, water and ethylene glycol mixture are poor heat transfer fluids, because the thermal conductivity of these fluids affects the heat transfer coefficient between the heat transfer medium and the heat transfer surface. Nanofluids have novel properties that make them potentially useful in many applications in heat transfer, including microelectronics, fuel cells, pharmaceutical processes, and hybrid-powered engines, engine cooling/vehicle thermal management, domestic refrigerator, chiller, heat exchanger, nuclear reactor coolant, in grinding, machining, in space technology, defense and ships, and in boiler flue gas temperature reduction, see Choi.[7] A very good collection of published papers on nanofluids can be found in the book by Das et al.[8] and in the review papers by Buongiorno[9] and Kakac and Pramuanjaroenkij.[10] Ishak et al.[11] have investigated the problem of MHD flow and heat transfer due to a stretching cylinder. Kuznetsov and Nield[12] have examined the Cheng-Minkowycz problem for natural convective boundary layer flow in a porous medium

*Author to whom correspondence should be addressed.
Email: elkabeir@yahoo.com
Received: 27 November 2014
Accepted: 2 January 2015

saturated by a nanofluid. Chamkha and Rashad[13] investigated the natural convection from a vertical permeable cone in nanofluid saturated porous medium with uniform heat and volume fraction fluxes. The boundary layer flow and Heat Transfer of a Nanofluid Past a stretching/shrinking sheet with a convective boundary condition is examined by Mansur and Ishak.[14] Chamkha et al.[15] have also studied the unsteady natural convection flow of a nanofluid over a vertical cylinder. Rashad et al.[16] studied the mixed convection boundary-layer flow past a horizontal circular cylinder embedded in porous medium filled with a nanofluid taking into account the thermal convective boundary condition. Recently, Kuznetsov and Nield[17] revisited the Cheng-Minkowycz problem in Ref. [12] by assuming that there is no nanoparticle flux at the plate and that the particle fraction value there adjusts accordingly. Rashad et al.[18] disscused the non-Darcy natural convection boundary-layer flow adjacent to a vertical cylinder embedded in a thermally stratified nanofluid saturated porous medium. The problem of unsteady flow over an impermeable contracting cylinder in a nanofluid is studied by Zaimi et al.[19] Ibrahim and Shanker[20] have studied the boundary layer flow and heat transfer over a non-isothermal exponentially stretching sheet due to a nanofluid. Ramesh et al.[21] have analyzed the MHD flow of maxwell fluid over a stretching sheet in the presence of nanoparticles.

All the above studies considered the no-slip flow boundary condition, but there are situations wherein such condition is not appropriate and should be replaced by the partial slip boundary conditions. Partial slips occur for most non-Newtonian liquids and nanofluids, such as emulsion suspensions, foams and polymer solutions. The liquids exhibiting boundary slip find applications in technological problems such as polishing of artificial heart valves and internal cavities. Rahman et al.[22] have studied the problem of hydromagnetic slip flow of water based nanofluids past a wedge with convective surface. Noghrehabadi et al.[23] have analyzed the development of the slip effects on the boundary layer flow and heat transfer of nanofluids over a stretching surface. Nandy et al.[24] investigated the slip effect on the MHD stagnation point flow and heat transfer of nanofluid over a stretching sheet. Das[25] studied the problem of nanofluid flow over a shrinking sheet with surface slip.

However, the objective of the present study is to analyze the effect of partial slip velocity on unsteady viscous flow and heat transfer of a nanofluid towards a contracting cylinder taking into account the convective boundary condition. Moreover, the effects of nanofluid Brownian motion, thermophoresis and Newtonian heating parameters on the boundary layer flow and heat transfer characteristics are examined. The governing boundary layer equations have been transformed into a system of non-linear ordinary differential equations using similarity variables. These have been numerically solved using an implicit finite difference scheme. The effects of governing parameters on the velocity, temperature and nanoparticle concentration are presented graphically, and the skin friction coefficient, heat and mass transfer rates are discussed quantitatively.

2. GOVERNING EQUATIONS

Consider the laminar flow of an incompressible nanofluid over an infinite cylinder in a contracting motion in the presence of slip velocity effect taking into account the thermal convective boundary condition. Figure 1 depicts a schematic view of the physical model and the coordinate system. z-axis is measured along the axis of the cylinder and the r-axis is measured in the radial direction. The flow is taken to be axi-symmetric about the z-axis. The diameter of the cylinder is assumed as a function of time with an unsteady radius $a(t) = a_0\sqrt{1-\beta t}$, where β is the constant of the expansion/contraction strength, t is time and a_0 is a positive constant. The temperature of the cylinder is taken into account as the result of a convective heating process which is characterized by a temperature T_f and a heat transfer coefficient h_f, and that the nanoparticle flux there is zero. When r tends to infinity, the ambient values of temperature and nanoparticle volume fraction attain constant values T_∞ and C_∞, respectively. It is assumed that the Navier's condition for the velocity slip is proportional to the local shear stress. For nanofluids, in cylindrical coordinates system of z and r the governing unsteady conservation of momentum, thermal energy and nanoparticles equations including the dynamic effects of nanoparticles can be written as follows[6, 17]

$$\frac{1}{r}\frac{\partial}{\partial r}(ru) + \frac{\partial w}{\partial z} = 0 \tag{1}$$

$$\frac{\partial u}{\partial t} + u\frac{\partial u}{\partial r} + w\frac{\partial u}{\partial z} = -\frac{1}{\rho}\frac{\partial p}{\partial x} + \nu\left[\frac{\partial^2 u}{\partial r^2} + \frac{1}{r}\frac{\partial u}{\partial r} + \frac{\partial^2 u}{\partial z^2} - \frac{u}{r^2}\right] \tag{2}$$

$$\frac{\partial w}{\partial t} + u\frac{\partial w}{\partial r} + w\frac{\partial w}{\partial z} = -\frac{1}{\rho}\frac{\partial p}{\partial z} + \nu\left[\frac{\partial^2 w}{\partial r^2} + \frac{1}{r}\frac{\partial w}{\partial r} + \frac{\partial^2 w}{\partial z^2}\right] \tag{3}$$

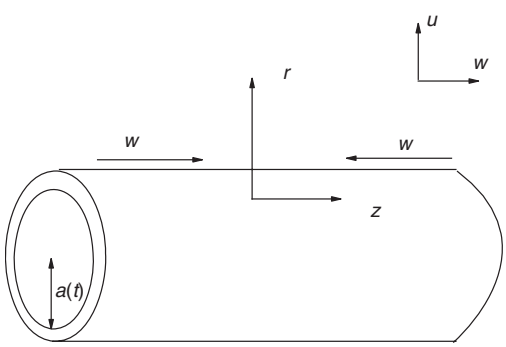

Fig. 1. The physical model and coordinate system.

ARTICLE

$$\frac{\partial T}{\partial t}+u\frac{\partial T}{\partial r}+w\frac{\partial T}{\partial z}=\alpha\left[\frac{\partial^2 T}{\partial r^2}+\frac{1}{r}\frac{\partial T}{\partial r}+\frac{\partial^2 T}{\partial z^2}\right]+\tau\left[D_B\left(\frac{\partial C}{\partial r}\frac{\partial T}{\partial r}+\frac{\partial C}{\partial z}\frac{\partial T}{\partial z}\right)+\frac{D_T}{D_B}\left[\left(\frac{\partial T}{\partial r}\right)^2+\left(\frac{\partial T}{\partial z}\right)^2\right]\right] \quad (4)$$

$$\frac{\partial C}{\partial t}+u\frac{\partial C}{\partial r}+w\frac{\partial C}{\partial z}=D_B\left[\frac{\partial^2 C}{\partial r^2}+\frac{1}{r}\frac{\partial C}{\partial r}+\frac{\partial^2 C}{\partial z^2}\right]+\frac{D_T}{T_\infty}\left[\frac{\partial^2 T}{\partial r^2}+\frac{1}{r}\frac{\partial T}{\partial r}+\frac{\partial^2 T}{\partial z^2}\right] \quad (5)$$

The initial and boundary conditions for this problem are;

$$\begin{aligned} &t<0:\ u=w=0,\quad T=T_\infty,\quad C=C_\infty \quad \text{at any } r,z\\ &t\geq 0:\ u=0,\quad w=-\frac{1}{a_0^2}\frac{4\nu z}{(1-\beta t)}+L\frac{\partial w}{\partial r}\\ &-k\frac{\partial T}{\partial r}=h_f(t)(T_f-T)\\ &D_B\frac{\partial C}{\partial r}+\frac{D_B}{T_\infty}\frac{\partial T}{\partial r}=0,\quad \text{at } r=a(t)\\ &w\to 0, T\to T_\infty,\quad C\to C_\infty \quad \text{at } r\to\infty \end{aligned} \quad (6)$$

where u and w are the velocity components along the r and z axes, respectively. T is the nanofluid temperature, C is the nanoparticle concentration, T_∞ and C_∞ are the constant temperature and nanoparticle volume fraction far from the surface of the cylinder, respectively. Further, ρ, k, ν and p are the density, thermal conductivity, kinematic viscosity and prssure of the nanofluid, while $\alpha=k/(\rho c)_f$ is the thermal diffusivity of the fluid and $\tau=(\rho c)_p/(\rho c)_f$ where $(\rho c)_f$ is the heat capacity of the fluid and $(\rho c)_p$ is the effective heat capacity of the nanoparticle material. D_B is the Brownian diffusion coefficient, D_T is the thermophoretic diffusion coefficient. The physical quantity L is the slip length, and h_f is the convective heat transfer coefficient. For details of the derivation of Eqs. (1)–(5), one can refer to the papers by Buongiorno[9] and Nield and Kuznetsov.[17]

The governing Eqs. (1)–(5) subjected to the boundary conditions (6) can be expressed in a simpler form by introducing the following similarity transformations;[4,5]

$$\eta=\left(\frac{r}{a_0}\right)^2\frac{1}{1-\beta t},\quad u=-\frac{1}{a_0}\frac{2\nu}{\sqrt{1-\beta t}}\frac{f(\eta)}{\sqrt{\eta}}$$
$$w=\frac{1}{a_0^2}\frac{4\nu z}{1-\beta t}f'(\eta) \quad (7)$$
$$\theta(\eta)=\frac{T-T_\infty}{T_f-T_\infty},\quad \phi(\eta)=\frac{C-C_\infty}{C_\infty}$$

where η is the similarity variable, θ is the dimensionless temperature and ϕ is the dimensionless nanoparticle volume fraction. By employing the boundary layer approximations and the similarity variables (7), Eq. (1) is satisfied automatically and Eqs. (2)–(5) reduce to the following ordinary differential equations;

$$\eta f'''+f''+ff''-f'^2-S(\eta f''+f')=0 \quad (8)$$

$$\frac{1}{\Pr}(\eta\theta''+\theta')+f\theta'-S\eta\theta'+\eta(Nt\theta'\phi'+Nb\theta'^2)=0 \quad (9)$$

$$\eta\phi''+\phi'+Le(f\phi'-S\eta\phi')+\frac{Nt}{Nb}(\eta\theta''+\theta')=0 \quad (10)$$

and the boundary conditions (6) become

$$\begin{aligned} &f(1)=0, f'(1)=-1+\delta f''(1), \theta'(1)=-Nc[1-\theta(1)]\\ &Nb\phi'(1)+Nt\theta'(1)=0 f'(\eta)\to 0\\ &\theta(\eta)\to 0, \phi(\eta)\to 0 \quad \text{as } \eta\to\infty \end{aligned} \quad (11)$$

where a prime indicates differentiation with respect to η. Here, S is the unsteadiness parameter for the contracting cylinder showing the strength of contraction, Nb is the Brownian motion parameter, Nt is the thermophoresis parameter, Pr is the Prandtl number, Le is the Lewis number, δ is the slip parameter, and Nc is the Newtonian heating parameter (Biot number) which are defined respectively as;

$$S=\frac{a_0^2\beta}{4\nu},\quad Nb=\frac{\tau D_B C_\infty}{\nu},\quad Nt=\frac{\tau D_T(T_f-T_\infty)}{T_\infty\nu}$$
$$\Pr=\frac{\nu}{\alpha}, Le=\frac{\nu}{D_B},\quad \delta=\frac{2L}{a_0\sqrt{1-\beta t}} \quad (12)$$
$$Nc=\frac{h_f(t)a_0\sqrt{1-\beta t}}{2k}$$

It is important to note that as the convective parameter Nc increases, the heat transfer rates approaches the isothermal case. This statement is also supported by the first thermal boundary condition of Eq. (11), which gives $\theta(1)=1$ as $Nc\to\infty$. Also, it should be noted that the case $\delta=0$ corresponds to the case of no-slip at the cylinder surface of the boundary. In a case in which Nb and Nt are equal to zero, the present analysis reduces to the classical problem of flow and heat transfer due to a contracting cylinder in a viscous fluid (regular Newtonian fluid). Moreover, it is noted that most nanofluids analyzed large values of the Lewis number (Le > 1). For water nanofluids at room temperature with nanoparticles of 1–100 nm diameters, the Brownian diffusion coefficient D_B ranges from 4×10^{-4} to 4×10^{-12} m^{-2}/s, and, the ratio of the Brownian diffusivity coefficient to the thermophoresis coefficient for particles with diameters of 1–100 nm can be varied in the ranges of 0.02–2 for alumina, and from 2 to 20 for copper nanoparticles (see Buongiorno[9] for details). Hence, the variation of the nanofluids parameters in the present analysis is reported to vary in the mentioned range.

Table I. Comparison of the skin-friction coefficient $f''(1)$ with those of Zaimi et al.[6] by setting $f(1) = \gamma$ in the boundary conditions (1) for various values of S and γ for a regular Newtonian fluid ($Nb = Nt = 0.0$) at $\delta = 0.0$ and $Nc \to \infty$ (with no-slip boundary condidtions flow along isothermal contracting cylinder).

	Zaimi et al.[6]				Present results			
S	$\gamma = 0.1$	$\gamma = 1.0$	$\gamma = 1.5$	$\gamma = 2.0$	$\gamma = 0.1$	$\gamma = 1.0$	$\gamma = 1.5$	$\gamma = 2.0$
−4.0	3.8407	4.7879	5.3076	5.8240	3.8465	4.7942	5.3143	5.8305
−3.5	3.2990	4.2610	4.7857	5.3059	3.3048	4.2664	4.7921	5.3125
−3.0	2.7397	3.7255	4.2577	4.7833	2.7448	3.7308	4.2633	4.7893
−2.5	2.1466	3.1761	3.7205	4.2543	2.1517	3.1815	3.7256	4.2602
−2.0	1.4682	2.6012	3.1677	3.7150	1.4738	2.6064	3.1731	3.7199

The primary objective of this analysis is to estimate the parameters of engineering interest in fluid flow, heat and mass transport problems are the skin-friction coefficient, the reduced Nusselt number Nu_x, and reduced nanoparticle Sherwood number Sh_x. These parameters characterize the rates of the shear stress, heat and nanoparticle mass transfer, respectively. These can be defined in dimensionless form as follows:

$$C_f = \frac{\tau_w}{1/2\rho w_w^2} \tag{13}$$

$$Nu_x = \frac{a_0\sqrt{1-\beta t}q_w}{2k(T_f - T_\infty)} \tag{14}$$

$$Sh_x = \frac{a_0\sqrt{1-\beta t}q_m}{2D_B C_\infty} \tag{15}$$

where the shear stress τ_w, local heat flux q_w and local nanoparticle mass flux q_m from the contrating cylinder can be obtained, respectively from;

$$\tau_w = \mu\left(\frac{\partial w}{\partial r}\right)_{r=a(t)} = \frac{1}{a_0^3}\frac{8\nu\mu z}{(1-\beta t)^{3/2}}f''(1) \tag{16}$$

$$q_w = -k\left(\frac{\partial T}{\partial r}\right)_{r=a(t)} = \frac{2k}{a_0}\frac{(T_f - T_f)}{(1-\beta t)^{1/2}}[-\theta'(1)] \tag{17}$$

$$q_m = -D_B\left(\frac{\partial C}{\partial r}\right)_{r=a(t)} = \frac{2D_B}{a_0}\frac{C_\infty}{(1-\beta t)^{1/2}}[-\phi'(1)] \tag{18}$$

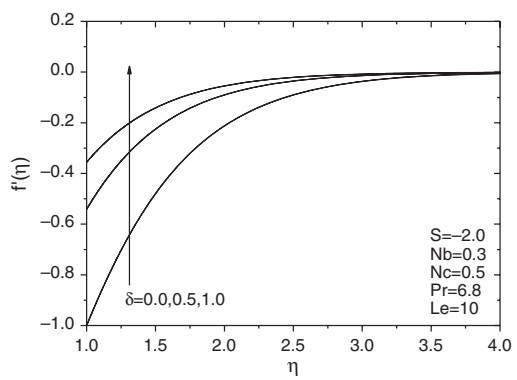

Fig. 2. Effects of δ and Nt on velocity profiles.

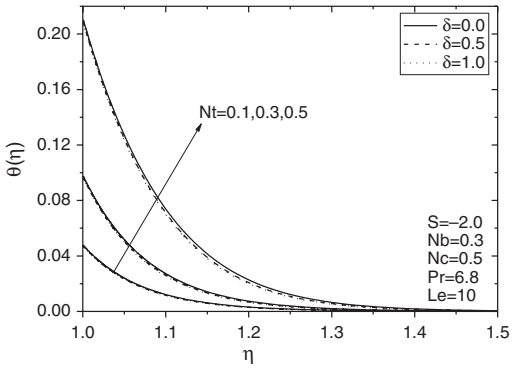

Fig. 3. Effects of δ and Nt on temperature profiles.

3. RESULTS AND DISCUSSION

In order to get a clear insight of the physical problem, numerical results are displayed with the help of graphical and tabulated illustrations. The system of Eqs. (8)–(10) with the boundary conditions (11) is solved numerically by means of an efficient, iterative, tri-diagonal implicit finite-difference method discussed previously by Blottner.[26] Since the changes in the dependent variables are large in the immediate vicinity of the cylinder while these changes decrease greatly as the distance away from the cylinder increases, variable step sizes in the η direction were used. The used initial step size in the η direction was $\Delta\eta_1 = 0.001$ and the growth factor was $K_\eta = 1.0375$ such that $\Delta\eta_n = K_\eta\Delta\eta_{n-1}$. This indicated that the edge of the boundary layer $\eta_\infty = 35$. The convergence criterion used was based on the relative difference between the current and the previous iterations which was set to 10^{-5} in the present work. To assure the validity and accuracy of the numerical method, the skin-friction coefficient results of the present study compared with those reported by Zaimi et al.[6] under some limiting case as shown in Table I, for various values of S and suction parameter γ and unsteadiness parameter S for a regular Newtonian fluid ($Nb = Nt = 0.0$) with no-slip boundary condition ($\delta = 0.0$) along along isothermal contracting cylinder ($Nc \to \infty$). It is found that

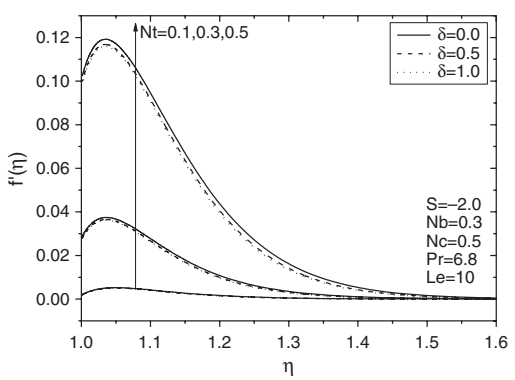

Fig. 4. Effects of δ and Nt on nanoparticles volume fraction profiles.

ARTICLE

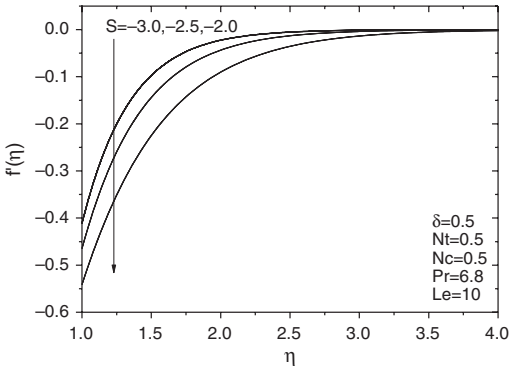

Fig. 5. Effects of S and Nb on velocity profiles.

our results are in excellent agreement with the previously published results.

In the present study, computations were carried out for various values of parameters, namely the slip parameter δ, unsteadiness parameter S, Brownian motion parameter Nb, thermophoresis parameter Nt, Biot number Nc and Lewis number Le. The value of the Prandtl number for the base fluid is kept at $Pr = 6.8$ (at the room temperature). The results of this parametric study are shown in Figures 2–9.

Figures 2–4 display the effects of slip factor δ and thermophoresis parameter Nt on the representative velocity f', temperature θ and volume fraction ϕ profiles, respectively. It can be seen that the velocity of the nanofluid f' increases while both the temperature θ and nanoparticle volume fraction ϕ decrease as the slip factor δ increases. Physically, this can be explained as the inclusion of the slip parameter can greatly change the surface drag force. This means that as the slip velocity at the cylinder surface increases, the momentum boundary layer thickness decreases and consequently, the nanofluid velocity increases under a slip condition at the boundary. On the other hand, an increase in the thermophoresis parameter Nt causes a significant rise in the temperature and volume fraction profiles. Also, the thermal and nanoparticle volume boundary layer thicknesses increase with the

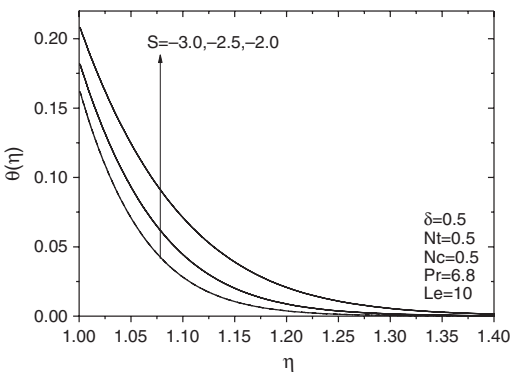

Fig. 6. Effects of S and Nb on temperature profiles.

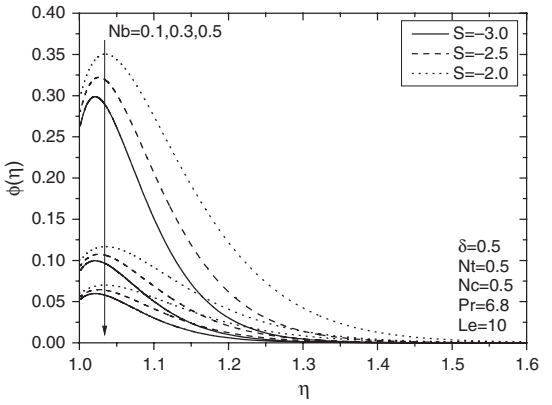

Fig. 7. Effects of S and Nb on nanoparticles volume fraction profiles.

increase of Nt. This can physically be explained according to the definition of the thermophoresis parameter Nt in Eq. (12) such that it represents the ratio of the nanoparticle diffusion, which is due to the thermophoresis effect, to the thermal diffusion in the nanofluid. Hence, following Buongiorno,[9] the solid particles in the fluid experience a force in the direction opposite to the imposed temperature gradient. Therefore, the particles tend to move from the hot region to the cold one.

Figures 5–7 depict the effects of the unsteady parameter S and the Brownian motion parameter Nb on the profiles of velocity f', temperature θ and the nanoparticle volume fraction ϕ, respectively. It is clear that an increase in the unsteady parameter S, causes an increase in the temperature and nanoparticle volume fraction profiles while the velocity profiles decreases. This can be explained as that according to the formulation in Eq. (12), the unsteadiness parameter S is the ratio of a defined cylinder radius variation speed to the viscous diffusion speed. Consequently, increasing the magnitude of S means lower viscous diffusion of the nanofluid. This yields reduction in the velocity profiles and increases in both the temperature

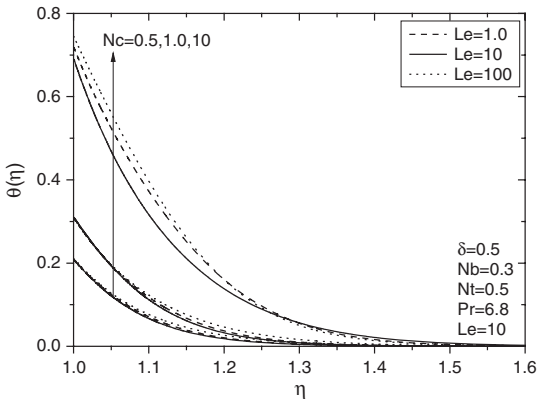

Fig. 8. Effects of Le and Nc on temperature profiles.

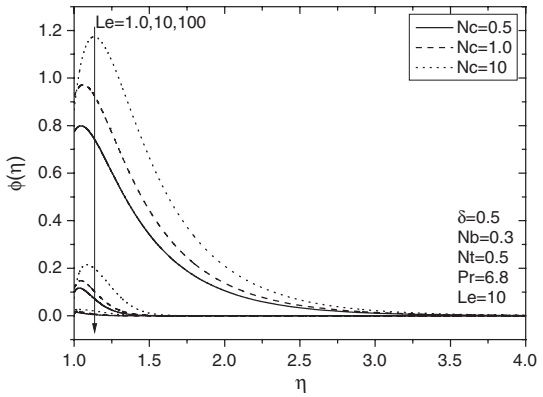

Fig. 9. Effects of Le and Nc on nanoparticles volume fraction profiles.

and nanoparticle volume fraction profiles. Furthermore, it is evident that the nanoparticle volume fraction ϕ and concentraion boundary layer thickness decreases significantly as the Brownian motion parameter *Nb* increases, whereas no effect occurs in the temterature profiles. This is due to the fact that the Brownian motion is proportional to the inverse of the size of the nanoparticles, see Buongiorno.[9] Therefore, the Brownian motion leads to reduction in the particle diameter which results in the decrease of the nanoparticle volume fraction.

Figures 8 and 9 show the temperature and nanoparticles volume fraction profiles for different values of the Lewis number *Le* and the Newtonian heating parameter *Nc* (Biot number), respectively. It is notcied that the increase of the Lewis number Le led to increase in the temperature profiles and to a pronounced decrease in the volume fraction profiles. This is due to the fact that there is a decrease in the nanoparticle volume fraction boundary layer thickness with the increase in the Lewis number. Moreovere, both the temperature and volume fraction rise with increasing the Boit number *Nc*. This is due to the fact that an increase in the Biot number *Nc* due to Newtonian heating of the cylinder surface causes an increase in the rate of convective heat transfer and nanoparticle mass fraction within the boundary layer region. In view of this explanation, a higher values of *Nc* produce strong surface convection which in turn, provides more heat to the cylinder surface and as a consequence, the temperature difference between the surface and the nanofluid intensifies.

The effects of governing parameters on the skin-friction coefficient, reduced Nusselt number Nu_x, and reduced nanoparticle Sherwood number Sh_x are respectively shown in Table II. From this table, it is noticed that as the slip

Table II. Local skin-friction coefficient C_f, local Nusselt number Nu_x, and the local Sherwood number Sh_x for different values of the physical parameters at Pr = 6.8.

Nt	δ	*Nb*	*S*	*Le*	*Nc*	$f''(1)$	$-\theta'(1)$	$-\phi'(1)$
0.1	0.0	0.3	−2.0	10	0.5	1.328587	0.3256453	−0.05958246
0.3	0.0	0.3	−2.0	10	0.5	1.328587	−0.1952822	0.8427125
0.5	0.0	0.3	−2.0	10	0.5	1.328587	−0.9925371	3.979718
0.1	0.5	0.3	−2.0	10	0.5	0.9178424	0.3257270	−0.05953538
0.3	0.5	0.3	−2.0	10	0.5	0.9178424	−0.1971476	0.8470517
0.5	0.5	0.3	−2.0	10	0.5	0.9178424	−1.005482	4.024632
0.1	1.0	0.3	−2.0	10	0.5	0.6446880	0.3257535	−0.05951599
0.3	1.0	0.3	−2.0	10	0.5	0.6446880	−0.1978394	0.8486619
0.5	1.0	0.3	−2.0	10	0.5	0.6446880	−1.010313	4.041390
0.5	0.5	0.1	−3.0	10	0.5	1.178232	−1.356518	15.739100
0.5	0.5	0.3	−3.0	10	0.5	1.178232	−1.356482	5.246242
0.5	0.5	0.5	−3.0	10	0.5	1.178232	−1.356487	3.147757
0.5	0.5	0.1	−2.5	10	0.5	1.071604	−1.194691	14.050630
0.5	0.5	0.3	−2.5	10	0.5	1.071604	−1.194589	4.683204
0.5	0.5	0.5	−2.5	10	0.5	1.071604	−1.194640	2.810025
0.5	0.5	0.1	−2.0	10	0.5	0.9178424	−1.005466	12.073700
0.5	0.5	0.3	−2.0	10	0.5	0.9178424	−1.005482	4.024632
0.5	0.5	0.5	−2.0	10	0.5	0.9178424	−1.005419	2.414648
0.5	0.5	0.3	−2.0	1.0	0.5	0.9178424	−0.9918432	3.966632
0.5	0.5	0.3	−2.0	10	0.5	0.9178424	−1.005482	4.024632
0.5	0.5	0.3	−2.0	100	0.5	0.9178424	−1.011303	4.146415
0.5	0.5	0.3	−2.0	1.0	1.0	0.9178424	−0.9981169	4.483553
0.5	0.5	0.3	−2.0	10	1.0	0.9178424	−0.9970712	4.489758
0.5	0.5	0.3	−2.0	100	1.0	0.9178424	−0.9833757	4.528114
0.5	0.5	0.3	−2.0	1.0	10	0.9178424	1.245354	1.009375
0.5	0.5	0.3	−2.0	10	10	0.9178424	1.339257	0.1993387
0.5	0.5	0.3	−2.0	100	10	0.9178424	1.378184	−0.6193712

ARTICLE

parameter δ increases, there is a rise in the rates of heat and nanoparticle mass transfer but a fall in the skin-friction coefficient. This is because the increase of the slip parameter leads to reduce the boundary resistance which in turn increases the nanofluid velocity. This yields a decrease in the wall shear stress and increases in the rates of heat and mass transfer at the cylinder surface. Moreover, as mentioned before, increasing the value of the thermophoresis parameter *Nt* causes increase in the thermal and nanoparticle volume boundary layer thicknesses. This yields an enhancement in the rate of nanoparticle mass transfer and a reduction in the rate of heat transfer as *Nt* increases. This is probably due to the fact that the thermophoresis parameter *Nt* is directly proportional to the heat transfer coefficient associated with the hot fluid, and it also plays a strong role in determining the diffusion of heat and nanoparticles concentration in the boundary layer. A similar behavior can be seen from Table I that the increasing of the Lewis number *Le* provides a considerable increase in the rate of volume fraction mass transfer while a slight increase in the rate of heat transfer is noticed with the increase in the Lewis number *Le*. This may be attributed to that fact that a higher value of Lewis number provides a lower nanoparticle volume fraction, this because the concentration at the cylinder surface is higher than that in the nanofluid. On the other hand, it is found that the rate nanoparticle mass transfer reduced strongly while the rate of heat transfer enhanced slightly as the Brownian parameter *Nb* increased. This is due to the fact that the Brownian diffusion promotes heat conduction. Also, the nanofluid is a two-phase fluid where the nanoparticles move randomly and increase the energy exchange rates. However, the Brownian motion reduces nanoparticles diffusion. Thus, the effects of variations of *Nb* and *Nt* on the rate of nanoparticle mass transfer are much higher than those effects on the rate of heat transfer. It is also nocited that the increase in the unsteady parameter *S* causes reduction in the magnitude of all of the skin-friction coefficient and rates of heat and mass transfer. Finally, it is observed that an increase in the Biot number *Nc* leads to increase in both of the heat and nanoparticle mass transfer rates. This may be attributed to the fact that as *Nc* increases, the intensity of Newtonian heating on the cylinder surface increases, which leads to increase the convective heat and nanoparticle mass transfer from the hot fluid on the lower of cylinder surface to the nanofluid on the upper surface.

4. CONCLUSION

In the present work, we have studied the effect of partial slip on unsteady viscous flow and heat transfer of nanofluid towards a contracting cylinder with Newtonian heating. The nanofluid model employed in the analysis includes the combined effects of Brownian motion and thermophoresis. The governing equations of the problem are converted into ordinary differential equations by using suitable similarity transformations. The similarity equations are solved numerically using an implicit finite-difference method. The results of the flow velocity, temperature and the nanoparticle volume fraction profiles are shown graphically for various values of the governing parameters. The obtained results for the local skin-friction coefficient, local Nusselt number and the local Sherwood number are displayed in tabular form to illustrate the effects the different physical parameters on them. It is concluded that that the skin-friction coefficient decreases with an increase in either of the slip parameter or the unseatdy parameter. In addition, the rates of heat and nanoparticle mass transfer reduce with an increase in the unseatdy parameter, whereas the opposite behavior happens with the increase of either the slip parameter or Biot number. Also, the rate of heat transfer decreases while the nanoparticle mass transfer rises with the increase of either of Lewis number or thermophoresis parameter. Furthermore, the rate of nanoparticle mass transfer decreases significantly while the rate of heat transfer increases slightly with the increase of Brownian motion parameter. Finally, the effects of variations of the Brownian motion and thermophoresis parameters on the changes in the rate of nanoparticle mass transfer are found to be more sufficient than those effects on the rate of heat transfer.

References and Notes

1. L. J. Crane, *Z. Angew. Math. Phys.* 21, 645 **(1970)**.
2. C. Y. Wang, *Phys. Fluids* 27, 1915 **(1984)**.
3. C. Y. Wang, *Phys. Fluids* 31, 466 **(1988)**.
4. A. Ishak, R. Nazar, and I. Pop, *Appl. Math. Model.* 2, 2059 **(2008)**.
5. T. Fang, J. Zhang, and Y. Zhong, *Commun. Nonlinear Sci. Numer. Simulat.* 17, 3124 **(2012)**.
6. W. M. K. A. Wan Zaimi, A. Ishak, and I. Pop, *Journal of King Saud University* 25, 143 **(2013)**.
7. S. U. S. Choi, Developments and Applications of Non-Newtonian Flows, ASME FED, edited by D. A. Siginer and H. P. Wang, 231/MD 66, 99 **(1995)**.
8. S. K. Das, S. U. S. Choi, W. Yu, and T. Pradeep, Science and Technology, Wiley, New Jersey **(2007)**.
9. J. Buongiorno, *ASME Journal of Heat Transfer* 128, 240 **(2006)**.
10. S. Kakac and A. Pramuanjaroenkij, *Int. J. Heat Mass Transfer* 52, 3187 **(2009)**.
11. A. Ishak, R. Nazar, and I. Pop, *Energy Conversion and Management* 49, 2365 **(2008)**.
12. D. A. Nield and A. V. Kuznetsov, *Int. J. Heat Mass Transfer* 52, 5792 **(2009)**.
13. A. J. Chamkha and A. M. Rashad, *Int. J. Numerical Methods for Heat and Fluid Flow* 22, 1073 **(2012)**.
14. S. Mansur and A. Ishak, *Abstract and Applied Analysis*, Article ID 350647 **(2013)**.
15. A. J. Chamkha, A. M. Rashad, and A. M. Aly, *Meccanica* 48, 71 **(2013)**.
16. A. M. Rashad, A. J. Chamkha, and M. Modather, *Computers and Fluids* 86, 380 **(2013)**.

17. A. V. Kuznetsov and D. A. Nield, *Int. J. Heat Mass Transfer* 65, 682 **(2013)**.
18. A. M. Rashad, S. Abbasbandy, and A. J. Chamkha, *ASME Journal of Heat Transfer* 136 **(2014)**.
19. K. Zaimi, A. Ishak, and I. Pop, *Int. J. Heat Mass Transfer* 68, 509 **(2014)**.
20. W. Ibrahim and B. Shanker, *J. Nanofluids* 4, 16 **(2015)**.
21. G. K. Ramesh, B. J. Gireesha, T. Hayat, and A. Alsaedi, *J. Nanofluids* 4, 100 **(2015)**.
22. M. M. Rahman, M. A. Al-Lawatia, I. A. Eltayeb, and N. Al-Salti, *International Journal of Thermal Sciences* 57, 172 **(2012)**.
23. A. Noghrehabadi, R. Pourrajab, and M. Ghalambaz, *International Journal of Thermal Sciences* 54, 253 **(2012)**.
24. S. K. Nandy and T. R. Mahapatra, *Int. J. Heat Mass Transfer* 64, 1091 **(2013)**.
25. K. Das, *Microfluid Nanofluid* 16, 391 **(2014)**.
26. F. G. Blottner, *AIAA Journal* 8, 193 **(1970)**.